Numerical Calculations for Smooth Circular Cylinder Flow at 3900 Reynolds Numbers with SST-IDDES Turbulence Model

Jiawei HE[*], Weiwen ZHAO, Decheng WAN[‡]

School of Naval Architecture, Ocean and Civil Engineering, Shanghai Jiao Tong University, Collaborative Innovation Center for Advanced Ship and Deep-Sea Exploration, Shanghai 200240, China
[*]Presenting author: jiaweihe@sjtu.edu.cn
[‡]Corresponding author: dcwan@sjtu.edu.cn
http://dcwan.sjtu.edu.cn

Abstract

The turbulent flow around a cylinder is simulated and analysed physically at Re =3900, by means of hybrid RANS-LES turbulence modelling approaches. The numerical investigations are conducted by using naoe-FOAM-SJTU, a viscous flow solver (naoe-FOAM-SJTU) which is developed and based on the popular open source toolbox OpenFOAM. To simulate the large separated flow in high Reynolds Numbers, turbulence closure has been chosen the Shear Stress Transport (SST) based Improved Delay Detached eddy simulation (IDDES). In the present study, the benefits of these hybrid approaches have been discussed for capturing the vortex dynamics and frequency modes. The coefficients of drag C_d and Strouhal number (S_t) were analyzed and compared with experimental results. Meanwhile，the boundary layer transition phenomenon and the flow characteristics were more accurately predicted. The good agreement validated the CFD solver naoe-FOAM-SJTU is applicable and reliable to study such problems.

Keywords: Circular Cylinder; Reynolds number; SST-IDDES; CFD.

Introduction

The fixed smooth cylinder-flow problem is considered to be a prominent research subject in computational fluid dynamics (CFD). Despite the reasonably simple geometry and grid-making, the very complex nature of this flow makes it extremely difficult to calculate. In this problem, the boundary layer, free-shear layers, and wake interact and the laminar-turbulent transition and boundary-layer separation move as Reynolds number varies. Also, several instabilities associated with the shear layers play an important role influencing the flow behavior in the different regimes. This particular issue is not only an academic challenge, but mainly an important engineering problem, being present in many fields, such as the vortex induced motion in the offshore industry. In this field, the vortex-induced vibrations of risers and vortex-induced motions of floating units stand out as a very important and current demand for which no complete and general solution has been developed.

As well known, the behavior of flow over a circular cylinder changes dramatically with the changes of Reynolds number. At low Reynolds number, the flow is laminar. While in region with higher Re, the turbulence appears. With increasing Reynolds number, the onset of transition moves upstream towards the separation point and, simultaneously, the large-scale vortices are formed closer to the base of the cylinder. The flow over a cylinder has been the subject of various experimental[1–3] and numerical studies[4–11]. Though，Kravchenko et al[5]

argued that the experiment of Lourenco and Shih[3] might have been contaminated by external disturbances which led to premature transition of the shear layers and thus to a shorter recirculation bubble. Nevertheless，the majority of the computational studies with CFD for Re =3900, mainly chosen the experimental data of Lourenco and Shih and Ong and Wallace. Dong [7] investigated the near wake flow of a circular cylinder with PIV and direct numerical simulation (DNS) at Re=3900/4000 and 10 000. They present a PIV/DNS comparison of mean and turbulent contour maps and focus on shear layer instability with their DNS data. WANG[12] has developed a finite-volume TVD numerical model to simulate an unsteady incompressible flow around a circular cylinder for subcritical Reynolds numbers of 1000, 3900 and 1×10^4. The method presented by WANG is validated by comparing with the available experimental data and numerical results. Charles Mockett [8] presented for the detached-eddy simulation (DES) of the flow around a circular cylinder at a high sub-critical Reynolds number(1.4×10^5). Good comparability with PIV experimental field data is facilitated by the confined and clearly-defined geometry, although some uncertainty remains regarding the free stream turbulence intensity. The combination of DES with an appropriate low-dissipative hybrid numerical convection scheme and high temporal resolution delivers excellent agreement with the experiment for the time and phase- averaged fields as well as the spectral content. Krishnan [13] used DES97 and DDES to predict the massively separated flow around a circular at Reynolds numbers based on the cylinder diameter and freestream velocity of 1.4×10^5 and 8×10^6. The DES97 and DDES predictions are in reasonable agreement with experimental measurements of the pressure coefficient. In a numerical experiment the possibility to influence the shear layer dynamics comes through the span-wise domain size chosen, the boundary conditions. Enforced the numerical errors inherent to the schemes used, the underlying grid.

The main objective of the present paper is to help building confidence of SST-IDDES turbulence model for massively separated flows. The recent publications by several authors of numerical simulations of the cylinder flow at Re=3900 led us to choose this case for the validation of SSTIDDES method in our solver. Flow around a cylinder at subcritical Reynolds number (*Re*=3900) was extensively studied numerically. It has become a benchmarking case and good agreements for mean stream-wise velocity obtained at both near wake and far downstream compared with the experimental data. To systematically validate the performance of SST-IDDES, the widely used hybrid RANS/LES model DDES is also presented in this paper for comparison.

Turbulence Modeling

Spalart[14]proposed the DES Detached Eddy Simulation approach to bridge the gap between RANS and LES. DES is a promising concept that could enable full scale engineering applications at high Reynolds number to be computed within the resources available today or in the near future[15]. To address this drawback, delayed-detached eddy simulation (DDES) modifies the character length scale to protect the RANS region from being prematurely switched into LES region. However, this modification is still incapable of completely preventing the occurrence of MSD problem[16]. In addition, several variants of the DES model, like Delayed DES (DDES) and Improved DDES (IDDES) have been proposed with rather different characteristics, making model selection and interpretation of results challenging.

SST-DDES

SST-DDES is a hybrid Reynolds-Averaged Navier-Stokes (RANS) - Large Eddy Simulation (LES) method. It utilizes sub-grid scale model to handle the flow in the free shear flow area far away from the wall, and RANS's SST model is used to solve the flow in the boundary layer near the wall and other areas. This can guarantee the accuracy of LES solution, but also reduce the amount of calculation in the near-wall region of the boundary layer.The SST-DDES equations are briefly described at first. The governing equations of the SST DDES model are as follows:

$$\frac{\partial \rho k}{\partial t}+\frac{\partial(\rho u_j k)}{\partial x_j}=P_k-\rho k^{\frac{2}{3}}/l_{DDES}+\frac{\partial}{\partial x_j}\left[(\mu+\sigma_k\mu_t)+\frac{\partial k}{\partial x_j}\right] \quad (1)$$

$$\frac{\partial \rho \omega}{\partial t}+\frac{\partial(\rho u_j \omega)}{\partial x_j}=\alpha\frac{\rho}{\mu_t}P_k-\beta\rho\omega^2+\frac{\partial}{\partial x_j}\left[(\mu+\sigma_\omega\mu_t)+\frac{\partial \omega}{\partial x_j}\right]+2(1-F_1)\rho\sigma_{\omega 2}\frac{\nabla k\cdot\nabla\omega}{\omega} \quad (2)$$

where F_1 and F_2 is a blending function which is defined as:

$$F_1=\tanh(\arg_1{}^4) \quad (3)$$

$$\arg_1=min\left[max\left(\frac{\sqrt{k}}{C_\mu\omega d_w},\frac{500v}{{d_w}^2\omega}\right),\frac{4\rho\sigma_{\omega 2}k}{CD_{k\omega}{d_w}^2}\right] \quad (4)$$

$$CD_{k\omega}=ax\left(2\rho\sigma_{\omega 2}\frac{\nabla k\cdot\nabla\omega}{\omega},10^{-10}\right) \quad (5)$$

$$F_2=\tanh(\arg_2{}^2) \quad (6)$$

$$\arg_2=max\left(\frac{2\sqrt{k}}{C_\mu\omega d_w},\frac{500v}{{d_w}^2\omega}\right) \quad (7)$$

Here d_w is the distance to the nearest wall. The production term P_k in Equation (1) reads as follows:

$$P_k=min\left(\mu_t S^2,10\cdot C_\mu\rho k\omega\right) \quad (8)$$

$$\mu_t=\rho\frac{a_1\cdot k}{max(a_1\cdot\omega,F_2\cdot S)} \quad (9)$$

The DDES length scale in Equation (1) reads as follows:

$$l_{DES}=\min\{l_{RANS},C_{DES}h_{max}\} \quad (10)$$

$$l_{DDES}=l_{RANS}-\boldsymbol{f_d}\max\{0,l_{RANS}-C_{DES}h_{max}\} \quad (11)$$

$$l_{RANS}=\frac{\sqrt{k}}{C_\mu\omega} \quad (12)$$

$$C_{DES}=C_{DES1}\cdot F_1+C_{DES2}\cdot(1-F_1) \quad (13)$$

Here h_{max} is the maximum edge length of the cell. Finally, the empiric blending function f_d in is computed with the use of the following relations:

$$f_d=1-\tanh[(C_{d1}r_d)^{C_{d2}}] \quad (14)$$

$$r_d=\frac{\nu+\nu_t}{\kappa^2{d_w}^2\sqrt{0.5\cdot(S^2+\Omega^2)}} \quad (15)$$

Here S is the magnitude of the strain rate tensor and Ω is the magnitude of vorticity tensor.
The model constants read as follows:

$C_\mu=0.09$, $\kappa=0.41, a_1=0.31, C_{DES1}=0.78, C_{DES2}=0.6, C_{d1}=20, C_{d2}=3.$

All the constants are computed by a blend from the corresponding constants of the *k-ε* and *k-ω* model via $\alpha=\alpha_1\cdot F_1+\alpha_2\cdot(1-F_1)\alpha 2$ etc. :

$$\alpha_1=5/9\ ,\ \beta_1=0.075\ ,\ \sigma_{k1}=0.85\ ,\ \sigma_{\omega 1}=0.5$$

$$\alpha_2=0.44\ ,\ \beta_1=0.0828\ ,\ \sigma_{k2}=1\ ,\ \sigma_{\omega 2}=0.856$$

SST-IDDES

The simplified version of IDDES length scale is as follows:

$$l_{IDDES} = \tilde{f}_d d + \tilde{f}_d(1 - \tilde{f}_d)\psi C_{DES}\Delta \quad (16)$$

$$\tilde{f}_d = \max\{f_B, 1 - f_{dt}\Delta\} \quad (17)$$

The LES length-scale Δ is defined as:

$$\Delta = min\{C_w max[d_w, h_{max}], h_{max}\} \quad (18)$$

$$f_{dt} = 1 - \tanh[(C_{dt1} r_{dt})^{C_{dt2}}] \quad (19)$$

$$r_{dt} = \frac{\nu_t}{\kappa^2 d_w{}^2 \sqrt{0.5\cdot(S^2+\Omega^2)}} \quad (20)$$

$$f_B = min\{2e^{-9\alpha^2}, 1.0\} \quad (21)$$

$$\alpha = 0.25 - d_w/h_{max} \quad (22)$$

In addition to the model constants in Equations (18) the following constants are introduced in the model:

$$C_w = 0.15, C_{dt1} = 20, C_{dt2} = 3$$

The full version of SST-IDDES model equations is shown in paper of Gritskevich[17] (2012).

Computational Domain and Mesh

The sketch of the computational domain can be seen in Fig.1. The distance spans 20*D* in stream-wise direction, 10*D* in lateral and 3.14*D* in vertical direction, respectively. Structured grid generation is chosen in this case due to the simple geometry of the cylinder. As shown in Fig. 2, the mesh domain of 10*D* around the cylinder is generated with the O block grids. While the rest of mesh domain is generated with orthogonal hexahedral grids. The thickness of the first grid near the wall of the cylinder is set as $\Delta = 0.005D$, corresponding to approximately $y^+ = 1.5$. As indicated by Zhao[18] (2016) and Travin[19] (2000), grid is not convergent on DES and LES simulations, i.e., the finest grid didn't get the best agreement for all quantities compared with experiments. Finally, a mesh is generated with the total number of grid units being 1.4 million.

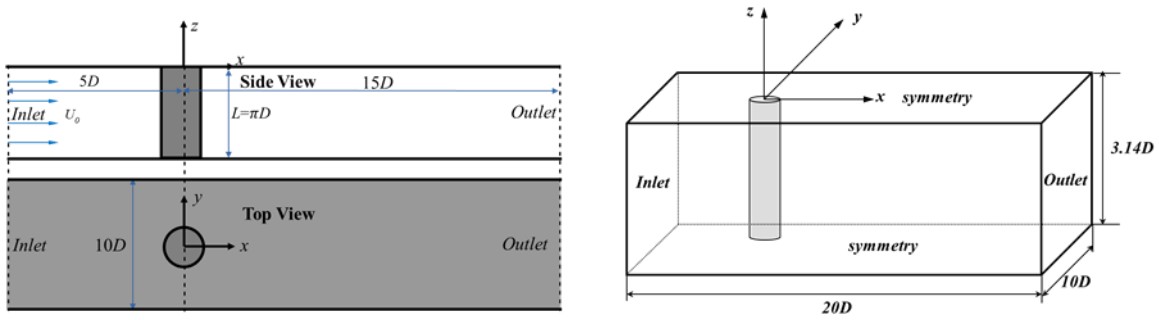

Fig. 1 Sketch of the computational domain

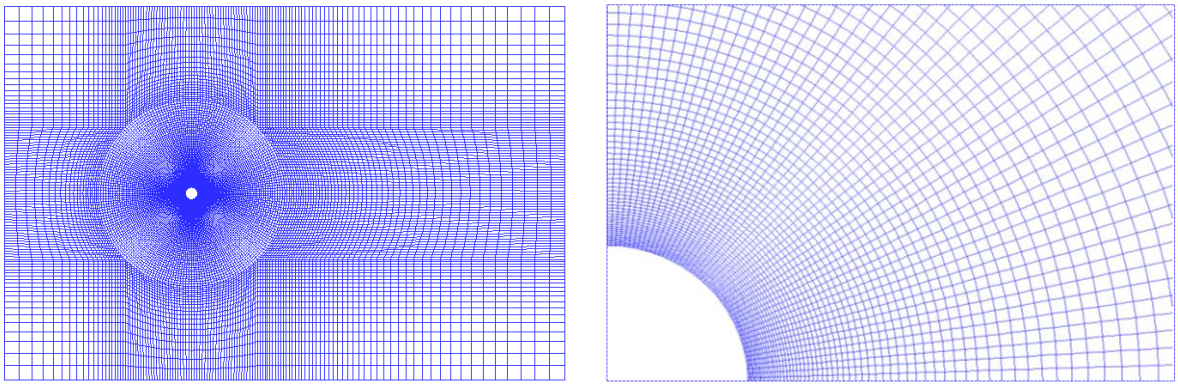

(a) Global mesh (b) Local mesh

Fig. 2 Global and local mesh for circular cylinder. (a) Global mesh. (b) Local mesh

Boundary Conditions and Other Computational Details

According to the physics feature of the computation domain, the boundary is marked as the inlet, the outlet, the sides, the bottom and top. The surface of the cylinder is considered as a no-slip wall. At the inlet boundary, a uniform incoming flow with velocity equal to the free stream velocity $U_\infty = 0.039m \cdot s^{-1}$is defined. At the outlet boundary, the pressure gradient is set equal to 0. The rest of the boundaries is defined as symmetry boundary for the reason of assuming that the height of the cylinder is infinite.

Discretization format

In this study, the governing equations are the three dimensional incompressible Navier-Stokes (N-S) equations. Since the SST-IDDES approaches are employed here. The governing equations are discretized using a finite volume method for solving the incompressible Navier–Stokes equations using solver naoe-FOAM-SJTU, with a newly implemented SST-IDDES turbulence model. The time discretization is done using second order implicit Euler scheme. A second order Gauss integration is used for spatial gradient calculations. The convection operator is discretized using a total variation diminishing (TVD) scheme.
The physics of the flow is considered as transient, incompressible and turbulent flow. Hence, we chose pimpleFoam as the solver for this case. pimpleFoam algorithm uses an inner PISO loop to get an initial solution, which is then under relaxed and corrected using an outer SIMPLE loop. This method enables unsteady simulations at Courant-Friedrichs-Lewy number (CFL) numbers larger than 1. In theory, very large CFL numbers could be maintained if a large number of SIMPLE correction loops were applied along with large under-relaxation factors. The equation of Courant-Friedrichs-Lewy (CFL) number is as follows:

$$\mathrm{CFL} = \frac{\Delta t U_\infty}{\Delta x} \tag{23}$$

A too large time step generally smears the solution, regardless of the grid resolution. Hence time step is chosen in such a way that CFL is less than 1.

Results and Discussions

Figure3 demonstrates the time histories of the present lift (C_l) and drag (C_d) coefficients for a period of 80 vortex shedding cycles.
The drag non-dimensional forces coefficient is given by:

$$C_d(t) = \frac{2F_x(t)}{\rho HDU^2} \tag{24}$$

Where $F_x(t)$ is the force in the in-line direction; U is the velocity of flow; ρ is the density of water; D, in this case, is the projected length (or characteristic diameter).
The lift non-dimensional forces coefficient is given by:

$$C_l(t) = \frac{2F_y(t)}{\rho HDU^2} \tag{25}$$

Where $F_y(t)$ is the force in the transverse direction; U is the velocity of flow; ρ is the density of water; D, in this case, is the projected length (or characteristic diameter).

The Reynolds number is defined as:

$$Re = \frac{UD}{\nu} \tag{26}$$

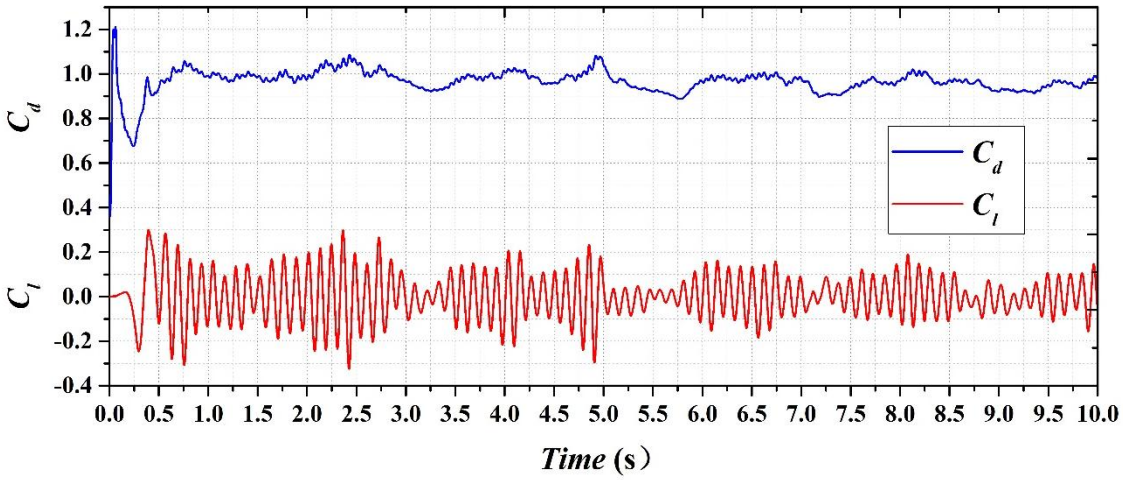

Fig. 3. Fluctuation of Coefficient of Drag(C_d) and Lift (C_l)Vs Time in second . Upper curves, C_d; lower, C_l

Initially the fluctuation goes on increases but after some time period it stabilities and fluctuates between the constant values. Further, the time-averaged drag coefficient is C_d calculated and listed in Table 1. The values obtained by the SST-DDES and SST-IDDES are in good agreement with the experimental data. the analysis of the vortex shedding frequency, or the Strouhal number (*St*), is obtained and given in Table 1. The values by the SST-DDES and SST-IDDES agree well with the experimental data. The present SST-IDDES and SST-DDES suggest a much longer recirculation bubble ($L_{rec}/D = 1.5$) than that indicated by experimental data of Lourenco and Shih[3](1993).

Table 1. Overall flow parameters of the flow past a circular cylinder, *Re*=3900

Data Source	C_d	$-C_{pb}$	S_t	L_{rec}/D	θ
PIV Exp. of Lourenco and Shih[3](1993)	0.99	0.88	0.215	1.33	89
DNS of Ma et al.[20] (2000)	0.84	-	0.220	1.59	-
SST-DES of Xu et al[9] (2010)	1.08	-	0.220	0.98	-
DNS of Frederic, Tremblay [10] (2002)	1.03	0.93	0.220	1.30	85.7
LES of Frederic, Tremblay [10] (2002)	1.14	0.99	0.210	1.04	87.3
LES of Kravchenko[5] (2000)	1.04	0.94	0.210	1.35	88.0
Present SST-DDES	0.99	0.83	0.207	1.27	87.1
Present SST-IDDES	0.97	0.87	0.215	1.20	86.5

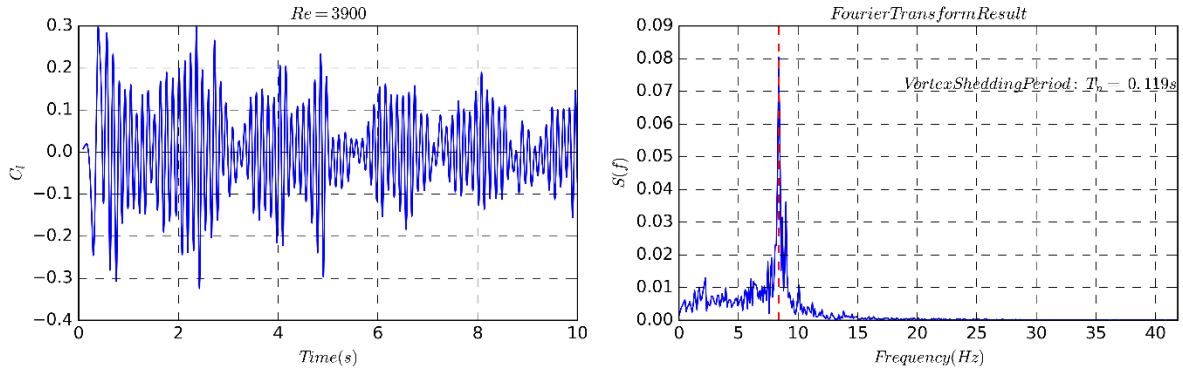

Fig. 4 Time history and Fourier transform result of Coefficient of Lift (C_l)

Figure 4 shows the time history and Fourier transform result of coefficient of lift (*Cl*). After the Fourier transform processing of data, the vortex shedding periods can be got with T_n=0.119s (i.e. the vortex shedding frequency f_n is equal to f_n =1/T_n=8.4 Hz.

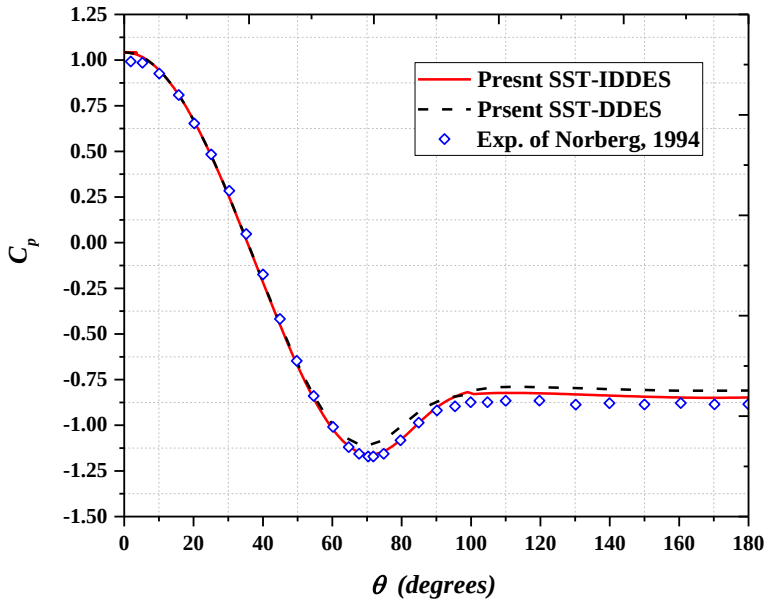

Fig.5 Time-averaged pressure coefficient on the surface of the cylinder with the experimental data and the SST-DDES results

Figure 5 Shows the time-averaged pressure distribution of SST-IDDES is reasonably below the SST-DDES result, and showing a good agreement with the experimental data[2].

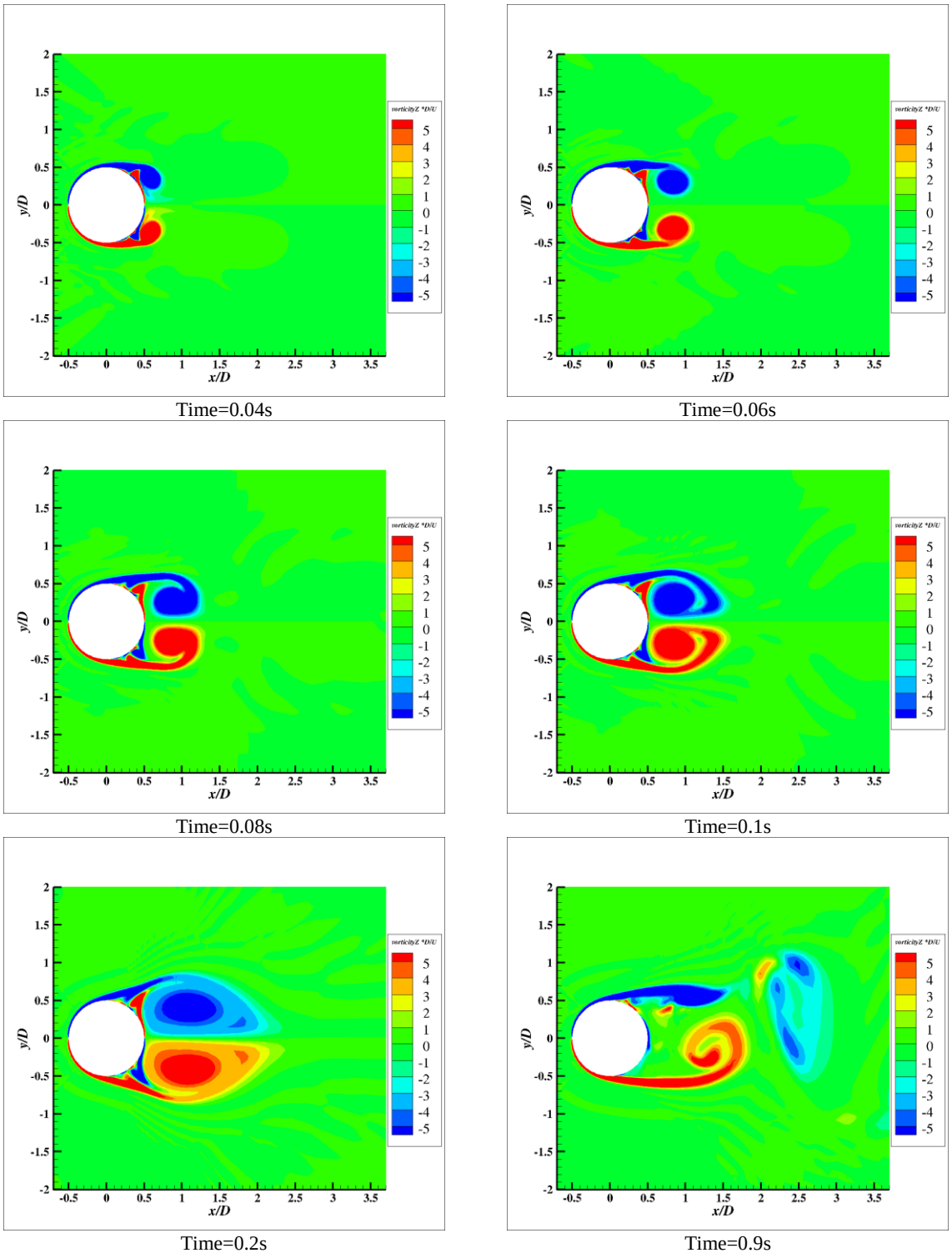

Fig. 6 The time evolution of instantaneous vorticity *Z* contour onto a horizontal plane (*z*=0)

Figure 6 shows the evolution of instantaneous vorticity *Z* at different time. The formation of the free shear layers from the cylinder surface took place identically for all runs. As the boundary layers from the upper and lower parts of the cylinder surface detach, free-shear layers are formed. This process is also displayed in Fig. 7. The separating shear layers behind the cylinder become unstable, and small-scale vortices can be clearly observed in the shear layers.

Figure 7 shows the iso-surface of the Q-criterion, flow past a circular cylinder with present SST-IDDES simulation. The slight difference vortex street pattern among each plane indicating the three dimensional turbulent structures.

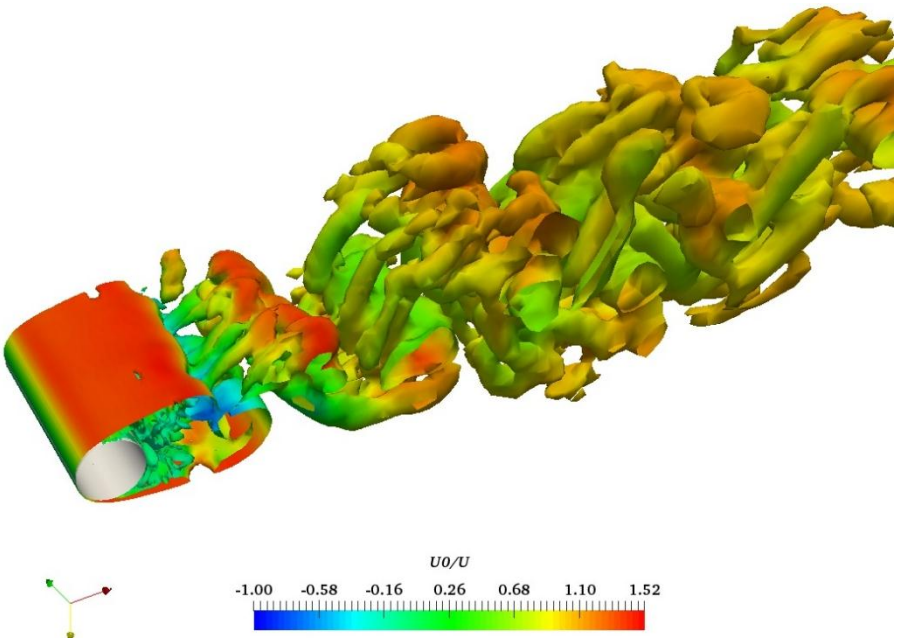

Fig. 7 Iso-surface of the Q-criterion, flow past a circular cylinder with present SST-IDDES simulation.

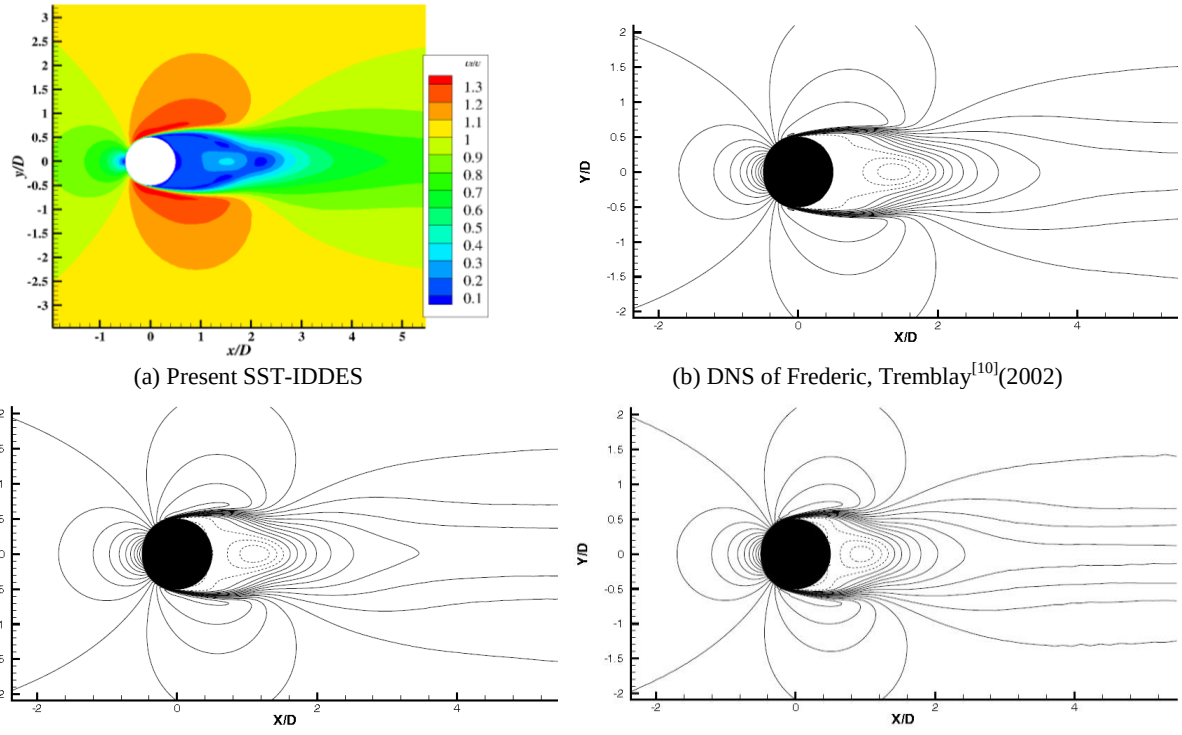

(a) Present SST-IDDES

(b) DNS of Frederic, Tremblay[10](2002)

(c) LES dyn of Frederic, Tremblay[10] (2002)

(d) LES smago of Frederic, Tremblay[10] (2002)

Fig. 8 Contours of mean velocity onto a horizontal plane (*z*=0)

Figure 8 shows contour and streamlines of mean velocity onto a horizontal plane.We again notice the shortening of the recirculation length obtained by our SST-IDDES computations as compared to the DNS result. We note once again the shorter recirculation bubble of the two LES computations by Frederic, Tremblay[10].

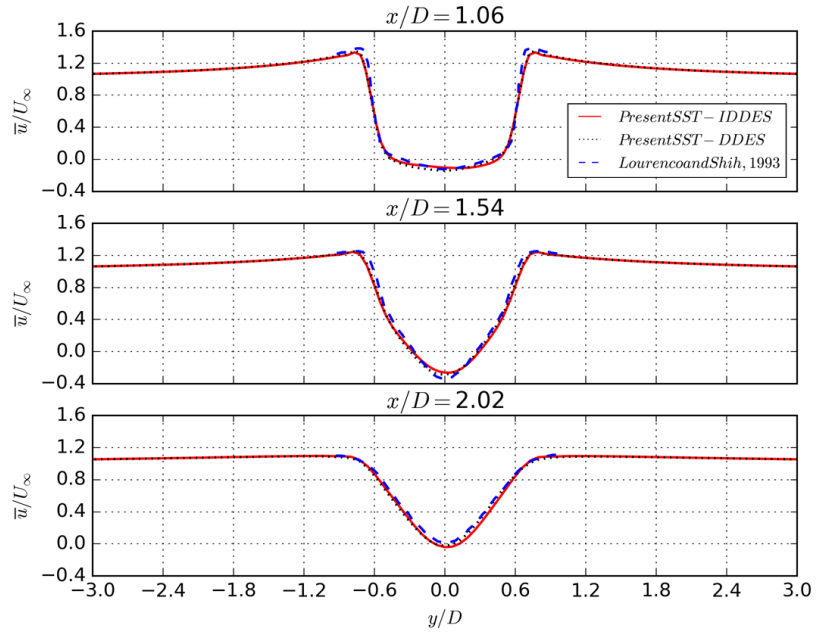

Fig. 9. Mean crossline velocities $\overline{u}/U_\infty$ in different cross-stream profiles of near wake behind the cylinder

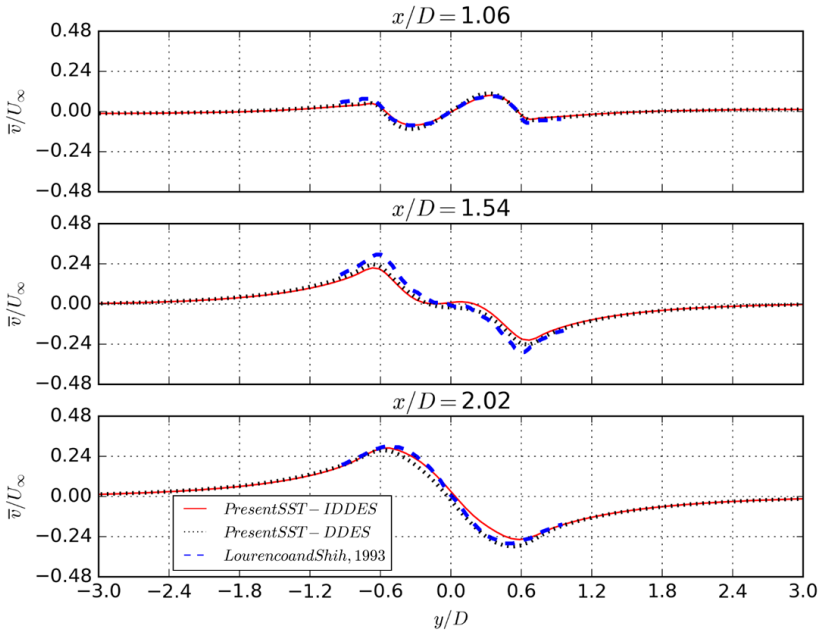

Fig. 10. Mean inline velocities $\overline{v}/U_\infty$ in different cross-stream profiles of near wake behind the cylinder

Figure 9 shows mean velocities in different cross-stream profiles of downstream. At *x/D* = 1.06, the axial velocity profile exhibits a typical U shape that many others have also found in their LES and DNS studies. At *x/D* = 1.54 and *x/D* = 2.02, both predictions yield V shaped profiles. These cross-stream profiles of the mean axial velocity for both meshes are consistent with the observations made earlier with regard to the length of the recirculation bubble. It has been discussed by Kravchenko[5] that the difference between a U shape and a V shape of the mean streamwise velocity profile in the near wake is mainly due to the shear layer dynamics

which affect this region. Figure 10 contains averaged over sufficient time inline velocities plots in series of cross-stream profiles along the downstream past the cylinder.

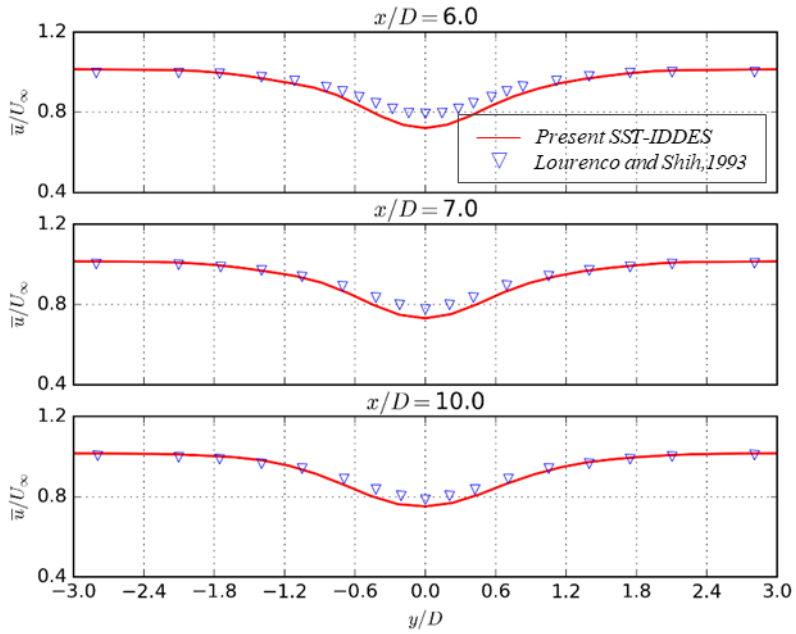

Fig. 11 Mean crossline velocities in different cross-stream profiles of near wake behind the cylinder

The normalized mean stream-wise velocity U/U_∞ in the far wake of the cylinder ($x/D \leq 10$) is plotted in Figure 11. Obviously, SST-IDDES didn't predicts the minimum value along the centerline of the cylinder. It could be due to the rather large grid spacing in the far wake of the cylinder.

Conclusion and Outlook

The separated turbulent flow around a circular cylinder is investigated using SST-IDDES. Some typical results, e.g., the mean pressure and drag coefficients, velocity Profiles and Strouhal number are calculated. A detailed validation of the SST-IDDES implementation for the turbulent flow around a circular cylinder has been conducted, with impressive levels of agreement achieved with experimental PIV data for both time-averaged and instantaneous quantities. In general, the prediction of SST-IDDES is satisfactory compared with the experiment data. Moreover, the hybrid RANS/LES models are able to simulate small turbulence structures and three dimensional effect even with limited computational meshes. The good agreement validated the CFD solver naoe-FOAM-SJTU is applicable and reliable to study such problems. Nevertheless, high Reynolds number (supercritical Re) flows are still challenging for the author to use present SST-IDDES models. Maybe more numerical try will need to be carried out in the near future.

Acknowledgements

This work is supported by the National Natural Science Foundation of China (51379125, 51490675, 11432009, 51579145), Chang Jiang Scholars Program (T2014099), Shanghai Excellent Academic Leaders Program (17XD1402300), Shanghai Key Laboratory of Marine Engineering (K2015-11), Program for Professor of Special Appointment (Eastern Scholar) at Shanghai Institutions of Higher Learning (2013022), Innovative Special Project of Numerical

Tank of Ministry of Industry and Information Technology of China(2016-23/09) and Lloyd's Register Foundation for doctoral student, to which the authors are most grateful.

References

[1] Ong, L., and Wallace, J. (1996) The velocity field of the turbulent very near wake of a circular cylinder, *Experiments in Fluids* **20**(6), 441–453.
[2] Norberg, C. (1994) An experimental investigation of the flow around a circular cylinder: influence of aspect ratio, *Journal of Fluid Mechanics* **258**(1), 287–316.
[3] Lourenco L, S.C. (1994) Characteristics of the plane turbulent near wake of a circular cylinder, Technical report TF-62, CTR Annual Research Briefs,NASA Ames / Stanford University.
[4] Parnaudeau, P., Carlier, J., Heitz, D., and Lamballais, E. (2008) Experimental and numerical studies of the flow over a circular cylinder at Reynolds number 3900, *Citation: Physics of Fluids* **20**(085101),1-14.
[5] Kravchenko, A.G., and Moin, P. (2000) Numerical studies of flow over a circular cylinder at ReD=3900, *Physics of Fluids* **12**(2), 403–417.
[6] Zhao, R., Liu, J., and Yan, C. (2012) Detailed Investigation of Detached-Eddy Simulation for the Flow Past a Circular Cylinder at Re=3900, Springer, Berlin, Heidelberg, 401–412.
[7] DONG, S., KARNIADAKIS, G.E., EKMEKCI, A., and ROCKWELL, D. (2006) A combined direct numerical simulation–particle image velocimetry study of the turbulent near wake, *Journal of Fluid Mechanics* **569**, 185–207.
[8] Mockett, C., Perrin, R., Reimann, T., Braza, M., and Thiele, F. (2010) Analysis of Detached-Eddy Simulation for the Flow Around a Circular Cylinder with Reference to PIV Data, *Flow, Turbulence and Combustion* **85**(2), 167–180.
[9] XU, C., CHEN, L., and LU, X. (2007) Large-Eddy and Detached-Eddy Simulations of the separated flow around a circular cylinder, *Journal of Hydrodynamics, Ser B* **19**(5), 559–563.
[10] Frederic, T. (2002) Direct and large-eddy simulation of flow around a circular cylinder at subcritical Reynolds numbers, Fakultät für Maschinenwesen,Thesis,1-146.
[11] Pereira, F.S., Vaz, G., Eça, L., and Girimaji, S.S. (2018) Simulation of the flow around a circular cylinder at Re=3900 with Partially-Averaged Navier-Stokes equations, *International Journal of Heat and Fluid Flow* **69**, 234–246.
[12] WANG, J. song (2010) Flow around a circular cylinder using a finite-volume TVD scheme based on a vector transformation approach, *Journal of Hydrodynamics* **22**(2), 221–228.
[13] Krishnan, V., Squires, K.D., and Forsythe, J.R. (2006) Prediction of the Flow Around a Circular Cylinder at High Reynolds Number, *44th AIAA Aerospace Sciences Meeting and Exhibit, 9-12 January 2006*, Reno, Nevada ,United States, 10765–10774.
[14] Spalart, P.. (2000) Strategies for turbulence modelling and simulations, *International Journal of Heat and Fluid Flow* **21**(3), 252–263.
[15] Menter, F.R., Kuntz, M., and Langtry, R. (2003) Ten years of industrial experience with the SST turbulence model, *Turbulence, Heat and Mass Transfer* **4**(1), 625–632.
[16] Menter, F., and Egorov, Y. (2005) A Scale Adaptive Simulation Model using Two-Equation Models, *43rd AIAA Aerospace Sciences Meeting and Exhibit*, Reston, Virigina, American Institute of Aeronautics and Astronautics, 1095–1107.
[17] Gritskevich, M.S., Garbaruk, A. V., Schütze, J., and Menter, F.R. (2012) Development of DDES and IDDES formulations for the k-ω shear stress transport model, *Flow, Turbulence and Combustion* **88**(3), 431–449.
[18] Zhao, WW., Wan, DC, and Sun, R. (2016) Detached-Eddy Simulation of Flows over a Circular Cylinder at High Reynolds Number, *Proceedings of the Twenty-Sixth (2016) International Ocean and Polar Engineering Conference* **96**(10–11), 1528–1536.
[19] Travin, A., Shur, M., Strelets, M., and Spalart, P. (2000) Detached-Eddy Simulations Past a Circular Cylinder, *Flow, Turbulence and Combustion* **63**(1/4), 293–313.
[20] MA, X., KARAMANOS, G.-S., and KARNIADAKIS, G.E. (2000) Dynamics and low-dimensionality of a turbulent near wake, *Journal of Fluid Mechanics* **410**, S0022112099007934.